# Further aspects of the piezospectroscopy of singly ionized zinc in germanium*

N. R. Butler† and P. Fisher‡
*Department of Physics, Purdue University, West Lafayette, Indiana 47907*
(Received 11 August 1975)

A study of the excitation spectrum of singly ionized zinc in germanium under very high signal-to-noise ratios has revealed the $A'$, $A''$, and $G$ lines of this acceptor; the latter line is extremely weak. A number of further features have been observed at stresses higher than those previously used. The most striking effect is the dramatic growth of the $G$ components under stress due to very strong interaction between the substates of the excited state of the $G$ line and those of the excited state of the $D$ line. This interaction also causes strong nonlinear effects in the stress dependence of the energies of the stress-induced components of the excitation lines. More reliable deformation-potential constants are obtained than those previously given.

## I. INTRODUCTION

In two previous papers[1,2] results were presented of a study of the piezospectroscopic effects of the excitation spectrum of singly ionized zinc in germanium. Since then the more extensive use of a quantitative stress cryostat,[3] with an improved technique[4] for mounting the samples, has yielded richer stress-induced spectra and more reliable values for the deformation-potential constants. The observations have been extended to higher stresses than those used before as the mounting technique permits more homogeneous strains to be obtained at high stresses. In addition, several other excitations have been observed, including the $G$ line,[5] thus giving this acceptor spectrum the same status as for other acceptors in germanium.[6]

The system of singly ionized zinc, $Zn^-$ in germanium presents several experimental advantages over that of a group-III impurity. First, the energy spacings of the excitation lines of $Zn^-$ are about four times larger[2,7] than the corresponding spacings of the group-III impurities.[8] Consequently, large enough perturbations can be applied to produce resolvable components but still enable the results to be compared with linear theory.[1,9] Secondly, the excitation lines occur at much shorter wavelengths than do those of the group-III impurities which translates the measurement to a region of the spectrum where the experimental conditions are better.

## II. EXPERIMENTAL PROCEDURE

In all cases but one, the samples used were the same as those described in II. All samples were prepared from ingots which were double doped with Zn and Sb at levels sufficient to give observable concentrations of $Zn^-$. More details of this are given in II. The samples were subjected to uniaxial compression by use of the quantitative stress cryostat described in Ref. 3. The technique which was developed to produce more homogeneous strains is described in Ref. 4. The spectrometer used to study the excitation spectra consisted of a linear wavelength drive E – 1 monochromator[10] equipped with a zinc-doped germanium detector.[11] The infrared beam was modulated at 1.4 kHz to maximize the signal-to-noise ratio. The output of the lock-in amplifier was encoded onto punch cards by a novel interface,[4] the data being processed by a computer which provided a precision plot of absorption coefficient vs photon energy. In order to obtain an extremely high signal-to-noise ratio, some spectra were recorded a number of times and computer averaged. In some cases, the parameters of the observed excitations, such as areas and energies of peaks, were determined from a curve-fitting program.[4]

## III. EXPERIMENTAL RESULTS AND DISCUSSION

### A. Zero-stress spectrum

The spectrum of $Zn^-$ in germanium is shown in Figs. 1, 2, and 3. In these figures, and those which follow, the samples are designated by their code number which permits comparison of the results with those presented in II. Figure 2 is the average of two scans of the higher-energy part of the spectrum of Fig. 1 expanded to show the weak lines more clearly. These four lines, labeled $A'$, $A''$, $A'''$, and $a$, were not observed previously for $Zn^-$, nor was the shoulder $C''$ although $a$ was observed under stress in II but not identified. The labeling of the $A$ lines is the same as that used for those of copper impurity in germanium.[12] There is some ambiguity involved in labeling these transitions since, for aluminum, Haller and Hansen[13] appear to have observed four $A$ lines, one of which is to the high-energy side of $A'$ and $A''$ and the other to the low-energy side. The energy spacings

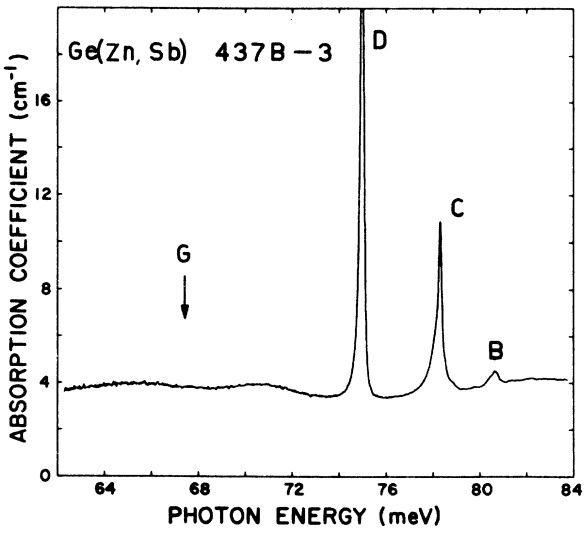


FIG. 1. Excitation spectrum of singly ionized zinc impurity in germanium. Liquid helium used as coolant. The energy of the $G$ line is deduced from Fig. 3.

of the present three $A$ lines are similar to those of the three higher-energy lines of Haller and Hansen. Figure 3 is the result of averaging 8 scans of the signal transmitted by the sample with 4 scans of the reference signal in the region of the spectrum at ~68 meV. The sample used was not the same as that of Figs. 1 and 2. The $G$ line has not been observed before, although some attempt was made to do so.[2] A fairly precise prediction of its energy was obtained by extrapolating the energies of its stress-induced components[5] to zero stress; this determined the energy range through which the multiple scans, summarized in Fig. 3, were to be made. Discussion of this is given in Sec. III B.

The energies and energy spacings for the spectrum of $Zn^-$ are given in Table I. The energies of the $B$, $C$, $C'$, and $D$ lines are those of II.[2,14] The ratios of the energy spacings to the average spacings of the corresponding lines of the neutral group-III impurities in germanium[8] are shown in the fourth column of Table I. It is seen that all the ratios are greater than four in agreement with the conjecture given in II to explain such ratios. It must be noted, however, that if the $A$ lines are identified with the sequence given by Haller and Hansen, the ratios for the spacings $A'$-$D$ and $A''$-$D$ become less than four, requiring that both conjectures given in II be invoked to understand the ratios.

### B. Effect of uniaxial stress

#### *1. Applied force along ⟨111⟩ axis*

The effect of a compressive force $\vec{F}$ on the spectrum of $Zn^-$ in germanium for $\vec{F} \| \langle 111 \rangle$ is shown in Figs. 4–7.[15] Figures 8 and 9 illustrate the stress dependence of the energies of the various components; in both these latter figures, the full lines

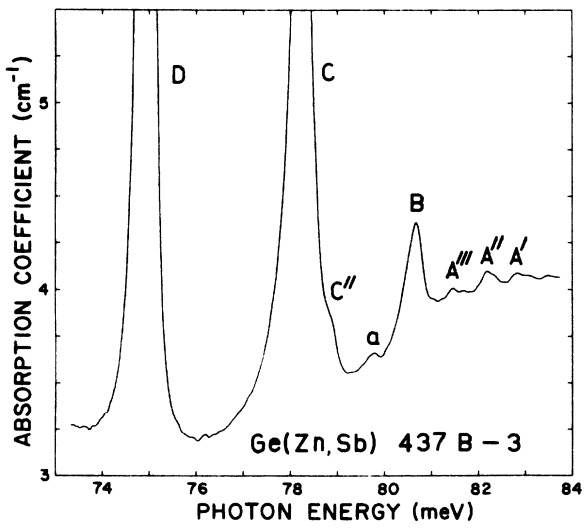


FIG. 2. A portion of the excitation spectrum of singly ionized zinc impurity in germanium expanded to show the weak high-energy lines.

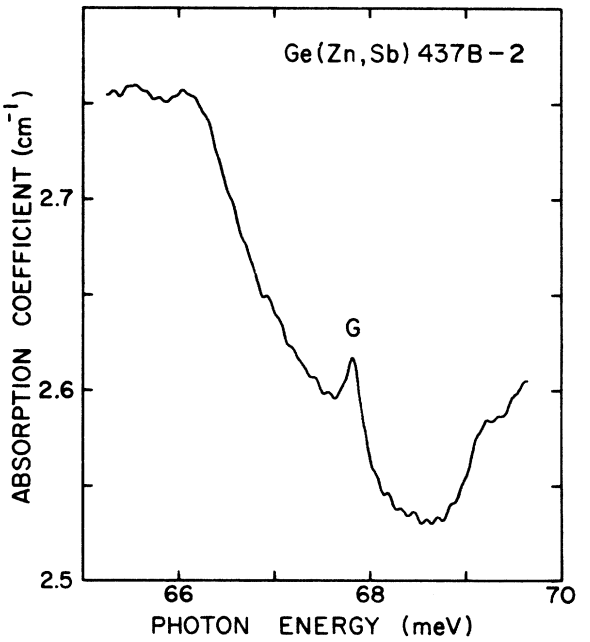


FIG. 3. The absorption of singly ionized zinc in germanium near the $G$ line. This is a computer-averaged spectrum obtained from 8 scans of the signal transmitted by the sample and 4 scans of the reference signal.

TABLE I. Energies and energy spacings of excitation lines of singly ionized zinc in germanium.

| Line | Energy (meV) | Spacing relative to $D$ line | Spacing relative to group III [a] |
|---|---|---|---|
| $A'$ | 82.79 ± 0.1 | 7.80 ± 0.1 | 4.17 ± 0.1 |
| $A''$ | 82.20 ± 0.1 | 7.21 ± 0.1 | 4.19 ± 0.1 |
| $A'''$ | 81.47 ± 0.1 | 6.48 ± 0.1 | ... |
| $B$ | 80.697 ± 0.011 [b] | 5.71 ± 0.02 | 4.12 ± 0.07 |
| $a$ | 79.78 ± 0.1 | 4.79 ± 0.1 | 4.32 ± 0.2 |
| $C''$ | 78.8 ± 0.2 | 3.8 ± 0.2 | ... |
| $C$ | 78.326 ± 0.002 [b] | 3.33 ± 0.01 | 4.40 ± 0.1 |
| $C'$ | 78.19 ± 0.04 [b] | 3.20 ± 0.05 | ... |
| $D$ | 74.994 ± 0.005 [b] | 0 | ... |
| $G$ | 67.80 ± 0.07 | 7.19 ± 0.07 | 4.25 ± 0.05 |

[a] Average spacings of group-III impurities in germanium obtained from Ref. 8.
[b] See Ref. 2. In this reference the energy of the $D$ line was reported incorrectly.

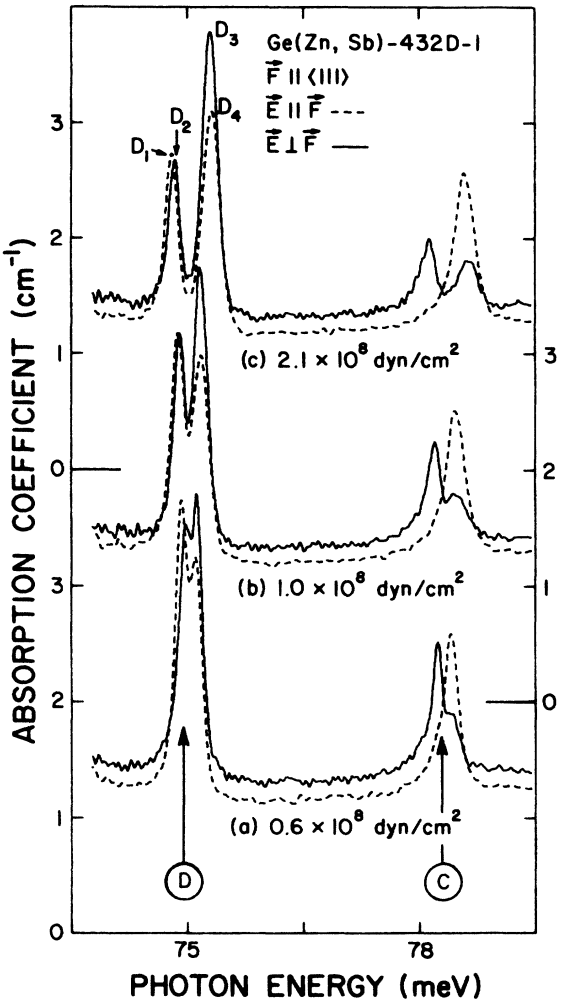


FIG. 4. A portion of the stress-induced spectrum of singly ionized zinc in germanium for three different stresses with a compressive force $\vec{F}$ parallel to ⟨111⟩ direction. Liquid helium used as coolant.

are smooth curves drawn through the data points. The origin of the labels $G_3$ and $G_4$ is discussed below. The intensity $I(G_4)$ of the $G_4$ component as a function of stress is also shown in Fig. 8. The data given in Fig. 9 are the result of three separate measurements made with two different samples using polarized radiation; in this figure no attempt has been made to distinguish the data points since these are numerous and fall close to each other.

Figure 4 shows the effect of small stresses on the $C$ and $D$ lines for a sample with a relatively low concentration of $Zn^-$. This result is to be compared with that of Fig. 8 in II and demonstrates unambiguously that, at stresses low enough to

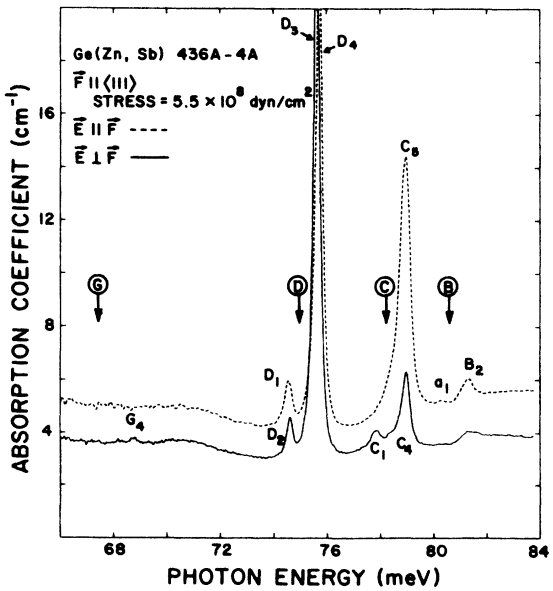


FIG. 5. Excitation spectrum of $Zn^-$ for $\vec{F} \parallel$ ⟨111⟩ for a stress of 0.55 kbar.

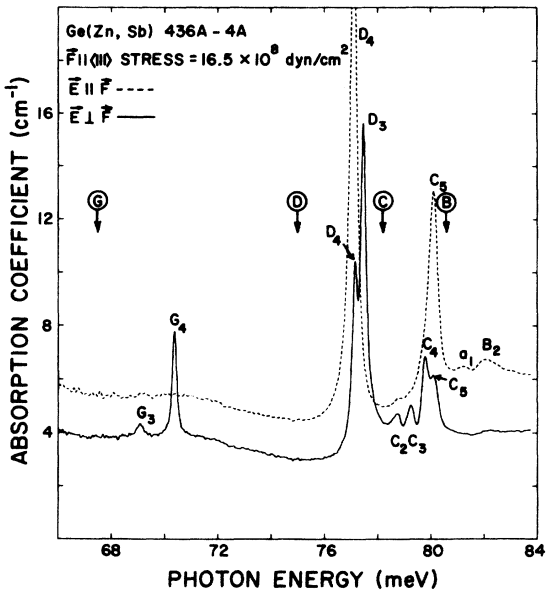


FIG. 6. Similar to Fig. 5 but for a stress of 1.65 kbar.

minimize depopulation effects, the $D_1$ component is stronger than the $D_4$ component. This clearly verifies the assignment given in II of the ordering of the ground-state sublevels for this direction of compression. The spectra of Figs. 5–7 are for higher stresses than those of Fig. 4 and have been obtained using a sample of higher $Zn^-$ concentration.

The spectra of Figs. 5–7 demonstrate a startling effect. Two sharp, clearly observable, $G$ components make their appearance in the range from ~68 to 71 meV and grow dramatically as the stress is increased. The nonlinear dependence of their energies on stress (see Fig. 8) and the strong stress dependence of their intensities clearly indicate that the states involved in these transitions are undergoing strong interactions with other states. The stress dependence of the energies of the $D$ components, shown in Fig. 9, implies that much of the interaction is between the states of the $G$ and $D$ excitations. This is an effect identical to that observed by Chandrasekhar *et al.*[16] for the components of lines 1 and 2 of the group-III acceptors in silicon. The calculations in this latter work predict that for two adjacent $\Gamma_8 \rightarrow \Gamma_8$ transitions several components can undergo drastic changes in intensity owing to interactions under stress. It is clear that the *stress-enhanced* components arise from the $G$ line, a $\Gamma_8 \rightarrow \Gamma_8$ transition.[8] The rapid decrease of the intensity of the $D_3$ component (see Figs. 5–7) and the growth of $G_4$ (see Figs. 5–8) implies that it is from $D_3$ that $G_4$ gains its strength. From Table III, Ref. 16 and I and II, it is deduced that, under a ⟨111⟩ compression, the sublevels of the final $\Gamma_8$ state of the $G$ line are ordered in the same way as those of the $\Gamma_8$ ground state. However, with this arrangement, the interaction described in Ref. 16 does not permit $G_3$ to be any larger than the extremely weak zero-stress parent line. In the case of $Zn^-$ in Ge though, for $\vec{F} \| \langle 111 \rangle$ there is very

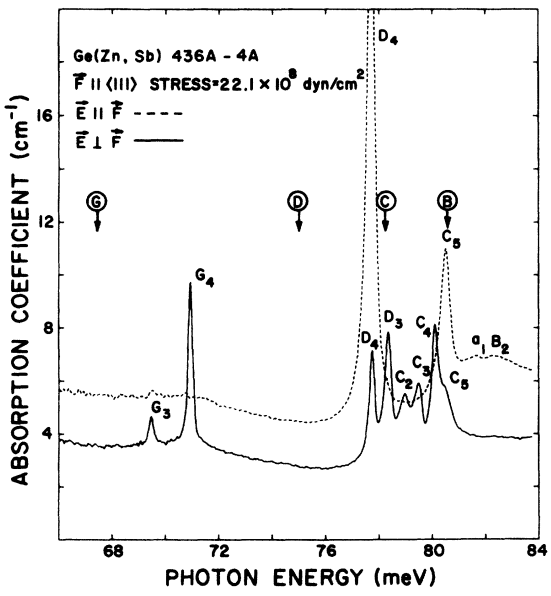


FIG. 7. Similar to Fig. 5 but for a stress of 2.21 kbar.

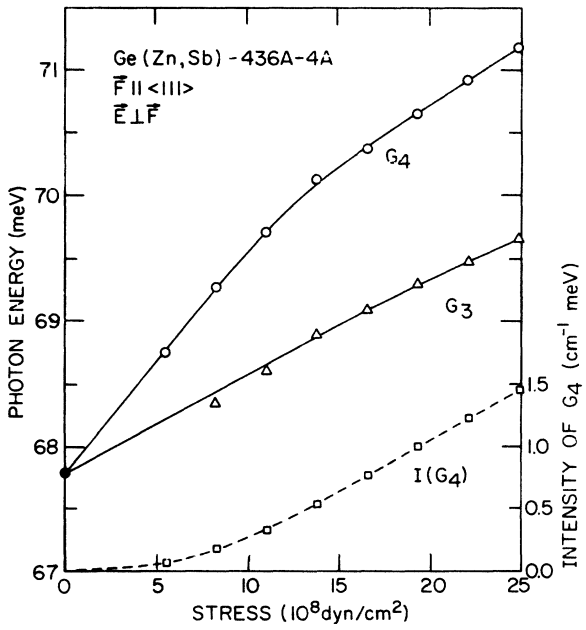


FIG. 8. Energies of the stress-induced components of the $G$ line versus stress for $\vec{F} \| \langle 111 \rangle$ and the intensity of the $G_4$ component as a function of stress.

little splitting of the final state of the $D$ line (see II), and hence the interaction between the $\Gamma_4$ substates of the final states of the $G$ and $D$ lines could be substantially larger than the corresponding effects for lines 1 and 2 of, for example, boron in silicon.[16] This interaction could account for the $G_3$ component of Figs. 5–8 but we have not carried out this analysis. The decrease in $D_3$ appears to be much larger than the combined growths of $G_3$ and $G_4$ implying that further interactions are involved. In Fig. 9, the stress dependence of the energies of the $D_3$, $D_4$, $C_3$, and $C_4$ components exhibit an inflection at a stress of ~$1.7\times10^9$ dyn/cm$^2$, suggesting that the sublevels of the final state of the $C$ line also are involved in the interaction.

It might be mentioned that the discovery of the $G$ components originated from the observation that at low stresses $D_1$ and $D_2$ crossed in energy as did $D_3$ and $D_4$,[17] suggesting that a lower-energy state was interacting with the final states of the $D$ line. This prompted measurements at higher stresses which showed the dramatic decrease in the $D_3$ component described above, in turn indicating that transitions to the lower-energy state involved in the interaction should be observed under stress even though the zero stress transition is too weak to be readily observed.

The large nonlinear shift of the $D_3$ component has separated it from the $D_4^{\perp}$ component (see Figs. 5–7 and Fig. 9), where the symbol $\perp$ means the radiation is polarized perpendicular to $\vec{F}$. This component was predicted in I but not reported in II since the stress used in II was not sufficiently large. The rapid decrease in the intensity of $D_3$ with increasing stress also contributes to the resolution of $D_4^{\perp}$.

The splitting of the ground state $\Delta'_{111}$ as a function of stress is shown in Fig. 10. The straight line is a least-squares fit to the data points and yields a value of $|\Delta'_{111}| = (1.95\pm0.07)\times10^{-9}|S|$, where $S$ is the stress in dyn/cm$^2$ and $\Delta'_{111}$ is in meV. This leads to $-2.32\pm0.09$ eV for $d'$ which is to be compared with $-2.18\pm0.06$ eV given in II. In view of the nonlinear splitting of the excited state of the $D$ line even at moderate stresses, it does not seem possible to obtain a reliable value for $d'_D$.

Proceeding as in II, a value of 0.23 was again obtained for the parameter $u_D$. This value was the average of six ratios of the areas of components $D_1$ and $D_2$ at low stresses. The areas were obtained from the curve fitting program. Low-stress values were used to minimize the effects produced by the unusually strong interaction between the $G$ and $D$ sublevels. A value of 0.12 is found for $u_D$ from the $D_3^{\perp}$, $D_4^{\perp}$, and $D_4^{\parallel}$ components. Here the symbol $\parallel$ means the radiation is polarized parallel to $\vec{F}$. Since $D_4^{\perp}$ has now been observed, it must be taken into account in estimating $u_D$. The value of 0.12 is larger than that obtained in II following

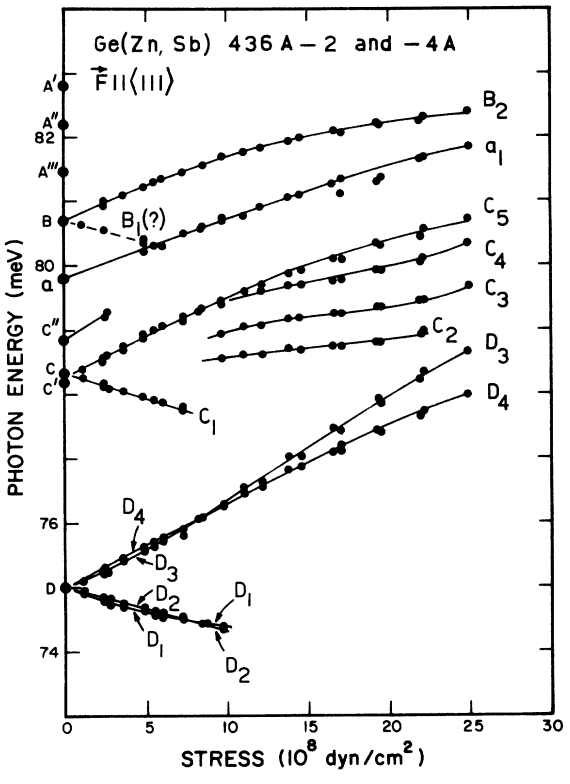


FIG. 9. Energies of the various stress-induced components of the $B$, $C$, and $D$ lines for $\vec{F}\parallel\langle111\rangle$ as a function of stress.

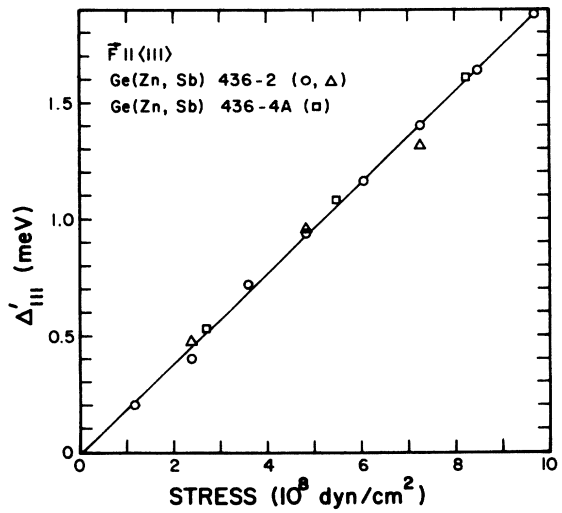


FIG. 10. Ground-state splitting of $Zn^-$ in germanium as a function of stress for $\vec{F}\parallel\langle111\rangle$.

the same procedure but is significantly lower than that determined from $D_1$ and $D_2$. This is not understood but should not be due to the interaction effects since the ratios used do not show any significant variation with stress at the stresses involved.

The data in Figs. 5–7 and Fig. 9 show that there are at least five $C$ components for $\vec{F}\|\langle 111\rangle$ instead of the three reported in II. The additional components are seen only for stresses $>10^9$ dyn/cm$^2$ and are only observed by virtue of their enhancement due to interactions. Further discussion of the $C$ line will be given below.

### 2. *Applied force along ⟨100⟩ axis*

The behavior of the $Zn^-$ spectrum under ⟨100⟩ compression is depicted in Figs. 11–13. The stress dependence of the energies of the various components is illustrated in Figs. 14 and 15. The results for the $B$, $C$, and $D$ lines are very similar to those of II except that an additional weak $C$ component is seen which has necessitated relabeling the highest-energy $C$ component. At a stress of 0.66 kbar (not shown) there is a clear indication of the presence of the $D_2^\perp$ component. The effect of depopulation of the upper ground state with strain was observed for this component over a limited range of stress.

For stresses >0.6 kbar, $D_2^\perp$ is sufficiently small not to influence the position of $D_3^\perp$. At stresses larger than ~1.2 kbar, $D_3^\perp$ shows a further decrease in intensity which is presumably not due to $D_2^\perp$ and suggests that $D_3^\perp$ is being affected by an interaction.

The stress dependences of $\Delta'_{100}$ and $\Delta^D_{100}$, the ground- and excited-state splittings, respectively, have been found in much the same manner as in II. Linear least-squares fits were made to $D_1$ and $D_4$ omitting the zero-stress energy of the $D$ line; these fits are represented by the straight lines in Fig. 15 and yield the stress dependence of $\Delta'_{100} + \Delta^D_{100}$. The values of $\Delta^D_{100}$ for the three data points in the range 0.6–1.0 kbar were obtained as the differences between the energies of $D_3$ and $D_4$. The average of these results gives $\Delta^D_{100} = 1.59 \times 10^{-9}|S|$ meV, with $S$ in dyn/cm$^2$ and an estimated error of 3%. From this value and that obtained for $\Delta'_{100} + \Delta^D_{100}$, it is found that $\Delta'_{100} = 1.84 \times 10^{-9}|S|$ meV, again with an estimated error of 3%. These values are larger than those given in Eqs. (3) and (4) of II. The present stress dependence of the energies of $D_1$ and $D_4$ are about 16% and 7% larger, respectively, than those found in II. The large difference between the two values for $D_1$ is under-

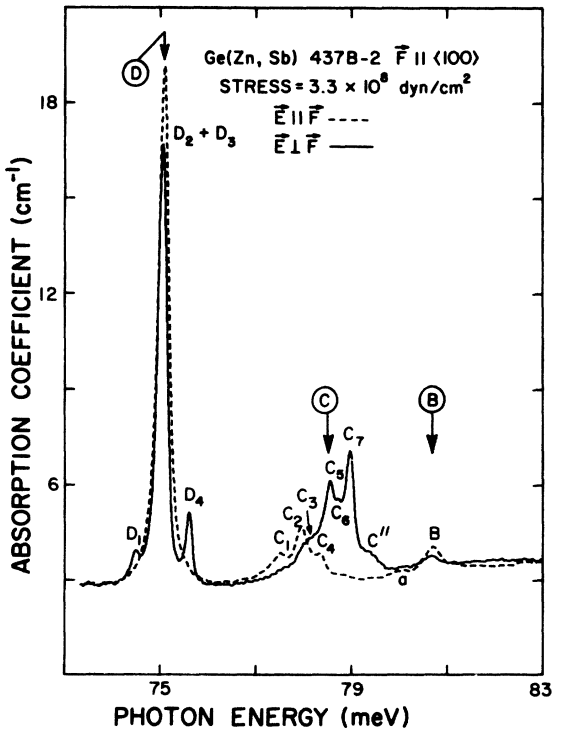


FIG. 11. Excitation spectrum of $Zn^-$ for $\vec{F} \| \langle 100\rangle$ for a stress of 0.33 kbar.

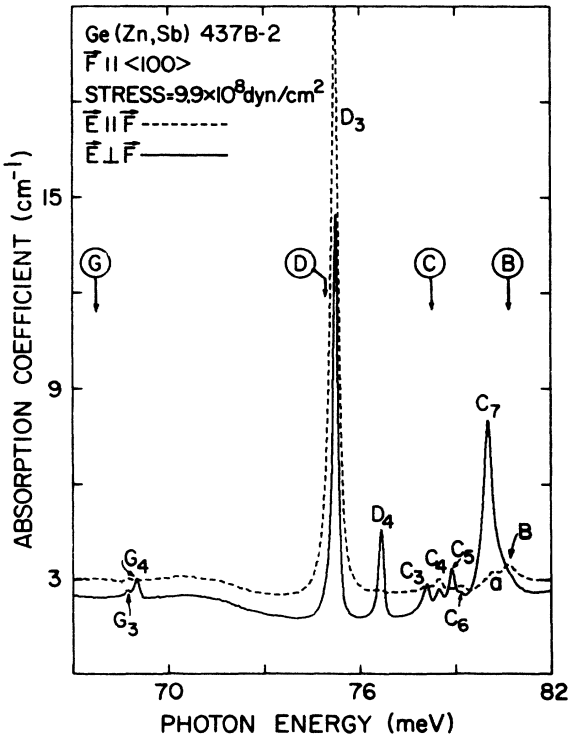


FIG. 12. Excitation spectrum of $Zn^-$ for $\vec{F} \| \langle 100\rangle$ for a stress of 0.99 kbar. The energy range has been extended compared with that of Fig. 11 in order to show the $G$ components.

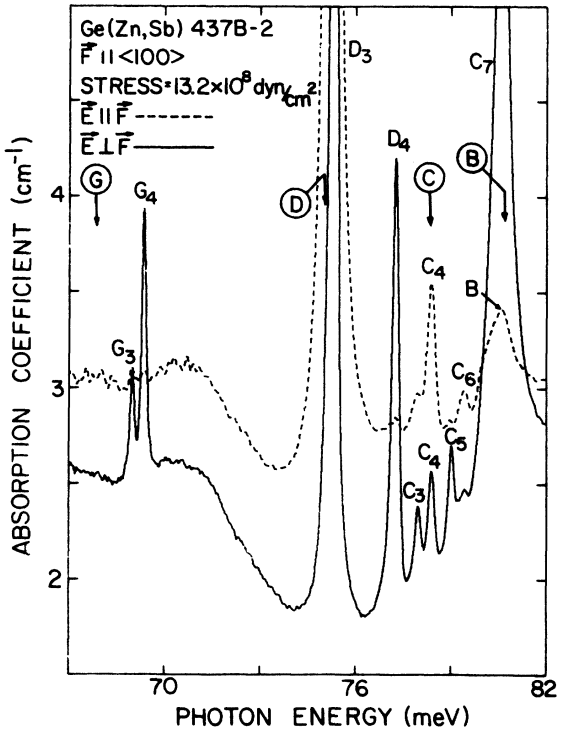


FIG. 13. Similar to Fig. 12 but at a higher stress and with an expanded ordinate to illustrate better the weak components and dramatize the $G$ components.

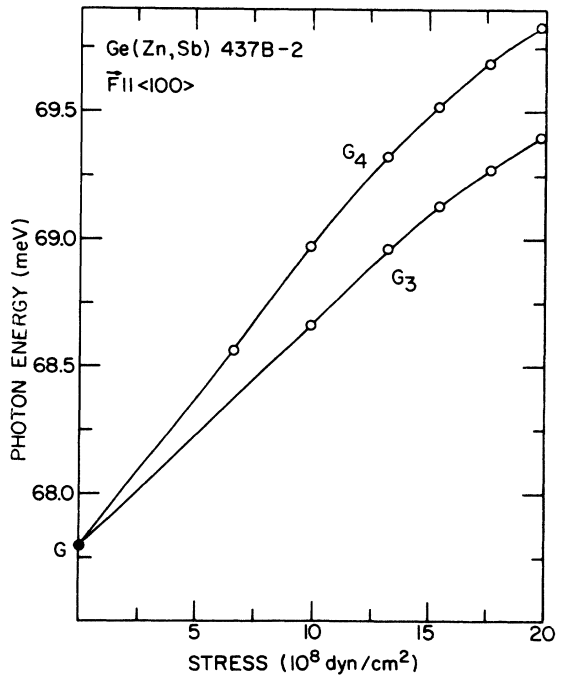


FIG. 14. Energies of the stress-induced $G$ components as a function of stress for $\vec{F} \parallel \langle 100 \rangle$.

standable since this component is always weak except at low stresses where it is not well resolved. The present data for $D_1$ exhibit less scatter than that seen in Fig. 15 of II. Part of this may be simply a manifestation of the procedure adopted in II to calibrate the strain jig measurements in terms of stress. A comparison of the spectra of Fig. 14 of II and Fig. 12 of the current work shows that in the latter a much more uniform stress has been achieved, suggesting that the present results are more reliable.

The results for $\Delta'_{100}$ and $\Delta^D_{100}$ give for the magnitudes of the deformation-potential constants $b'$ and $b'_D$ values of $0.75 \pm 0.02$ eV and $0.65 \pm 0.02$ eV, respectively. From these values one can predict the position of the $D_2$ component at a given stress. In the case of the spectrum, taken at 0.66 kbar, $D_2$ should occur at an energy of 75.01 meV, which is in good agreement with the position of a low-energy shoulder to $D_3^{\perp}$.

Figures 12 and 13 cover a larger energy range than does Fig. 11 and illustrate the growth of the $G$ components. Figure 13 is plotted with an expanded ordinate to illustrate the weak components and dramatize the $G$ components. The stress dependence of the energies of the $G$ components is displayed in Fig. 14. It is assumed that these grow in intensity at the expense of the $D_3^{\perp}$ component.

The intensities of the $D$ components can be used to obtain a value for $|v_D|$. Since $D_2^{\parallel}$ and $D_3^{\parallel}$ have not been resolved, it is necessary to consider those stresses for which $D_2^{\parallel}$ is essentially depopulated in order to compare $D_3^{\parallel}$ with $D_3^{\perp}$. In the

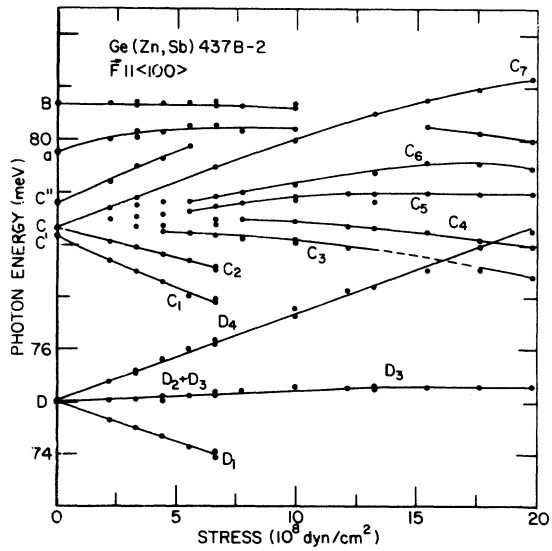


FIG. 15. Energies of the stress-induced $B$, $C$, and $D$ components for $\vec{F} \parallel \langle 100 \rangle$ as a function of stress.

analysis, $D_3^{\perp}$ was separated from the last vestiges of $D_2^{\perp}$ by the curve-fitting program. The ratio of $D_3^{\perp}$ to $D_3^{\parallel}$ is independent of depopulation effects and was found to have an average value of 0.385 for the spectra with stresses in the range 0.6–1.2 kbar. As already mentioned, at stresses larger than this range, $D_3^{\perp}$ shows an interaction effect. The ratios obtained gave a value of 0.25 for $|v_D|$ using the value of 0.23 obtained above for $u_D$. This result for $v_D$ confirms the tentative value given in II.

### 3. *Applied force along ⟨110⟩ axis*

Spectra obtained with $\vec{F}\|\langle 110\rangle$ are shown in Figs. 16–19. Unlike the other two orientations examined, the intensities of the stress-induced components for $E_{\perp}$ depend upon the direction of light propagation $\vec{k}$,[18] as may be seen from the figures. Figures 20 and 21 are plots of the energies of the various components as a function of stress. The present results for this direction of compression are very similar to those given in II except that now the region of the stress-enhanced $G$ components has been scanned for $\vec{k}\|\langle 110\rangle$ and two $G$ components observed (see Fig. 17). Also, a wider range of stresses is covered here, which enables the observation of several other new features.

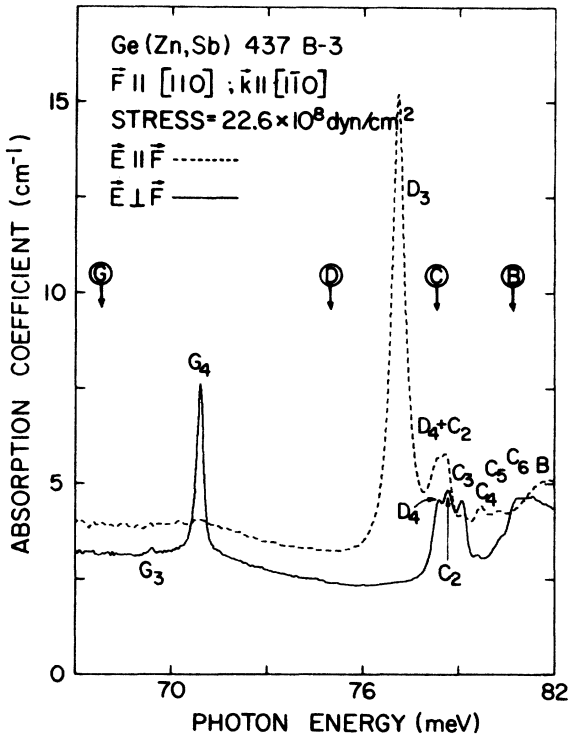


FIG. 17. Excitation spectrum of Zn$^-$ for $\vec{F}\|[110]$ and $\vec{k}\|[1\bar{1}0]$ with a stress of 2.26 kbar.

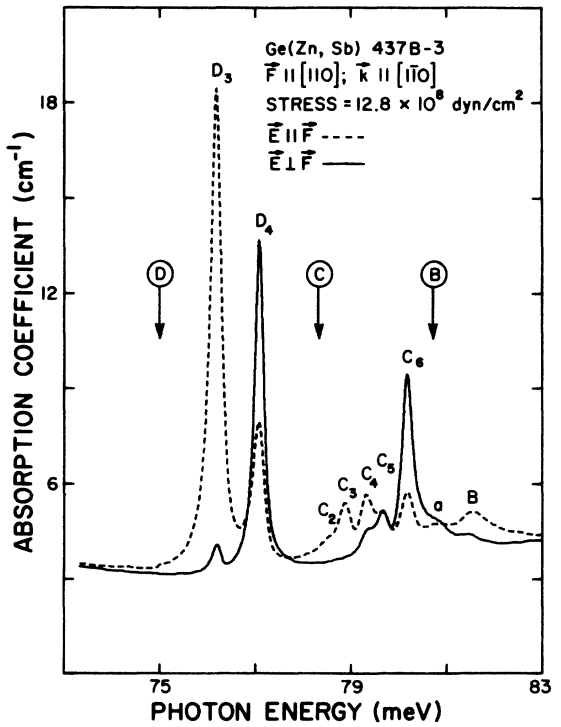


FIG. 16. Excitation spectrum of Zn$^-$ for $\vec{F}\|[110]$ and $\vec{k}\|[1\bar{1}0]$ with a stress of 1.28 kbar.

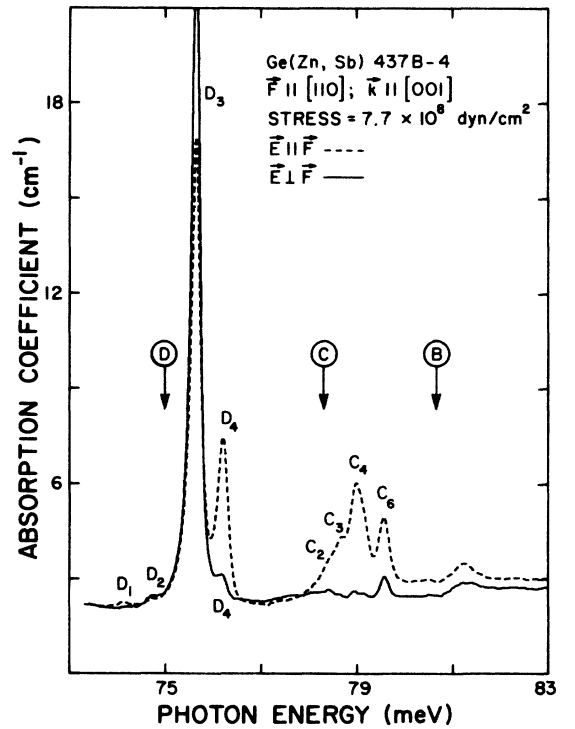


FIG. 18. Excitation spectrum of Zn$^-$ for $\vec{F}\|[110]$ and $\vec{k}\|[001]$ for a stress of 0.77 kbar.

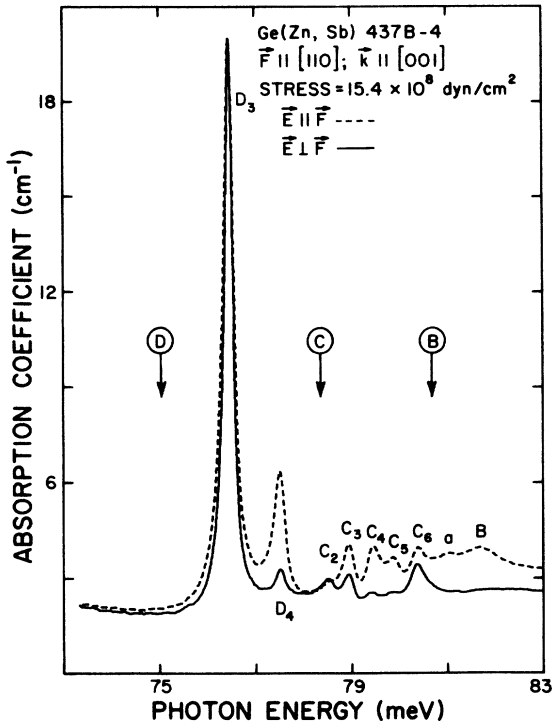


FIG. 19. Similar to Fig. 18 but with twice the stress.

One of these is the appearance of the $D_4^{\perp}$ component for $\vec{k}\|\langle 001\rangle$, which was predicted in II but not observed (see Fig. 20 of II and Figs. 18 and 19 of the present paper). In addition, at the higher stresses, more $C$ components appear than previously observed and many of the components show strong interaction effects for both their intensities and energies.

The present study, employing the quantitative stress cryostat, also enables the stress dependence of the various components for $\vec{F}\|\langle 110\rangle$ to be determined. The measured values of $\Delta'_{110}$ and $\Delta^D_{110}$ can then be compared with the values predicted using Eq. (29) of I. Figure 22 shows plots of $\Delta'_{110}$ and $\Delta^D_{110}$ as functions of stress. It should be noted that the data for these two quantities are not very reliable since at low stresses the lines are not well resolved, while at high stresses the $D_1$ and $D_2$ components vanish and $D_3$ and $D_4$ exhibit nonlinear shifts. The straight line labeled $\Delta'_{110}$ is drawn from the origin through the most reliable data point, that at $6.4\times10^8$ dyn/cm$^2$. This line gives $\Delta'_{110}=(1.80\pm0.09)\times10^{-9}\,|S|$ meV in good agreement with the value of $(1.92\pm0.07)\times10^{-9}|S|$ predicted from the values of $\Delta'_{111}$ and $\Delta'_{100}$ given above. It is interesting to note that, just as in the case of group-III acceptors in silicon,[16] the present values for $\Delta'_{111}$, $\Delta'_{100}$, and $\Delta'_{110}$ are the same within experimental error; $Zn^-$ in germanium may also exhibit stress isotropy.

In Fig. 22, the initial part of the line labeled $\Delta^D_{110}$ is a straight line drawn through the origin and the most reliable data point for this case, that at $10.2\times10^8$ dyn/cm$^2$. From this straight portion it is found that $\Delta^D_{110}=0.71\times10^{-9}|S|$ meV. It is difficult to estimate the error for this case since

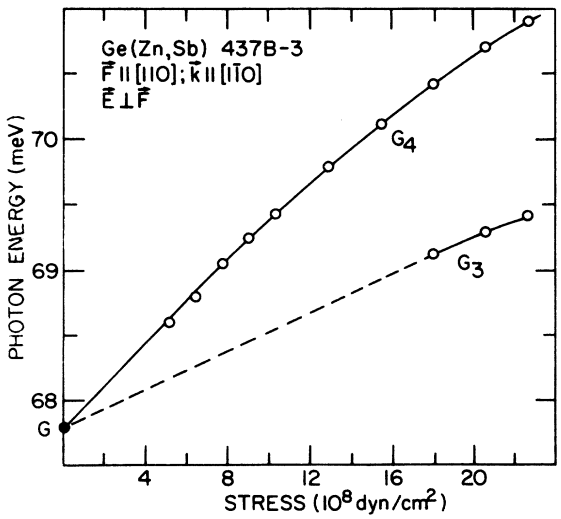


FIG. 20. Energies of the stress-induced $G$ components vs stress for $\vec{F}\|[110]$ and $\vec{k}\|[1\bar{1}0]$.

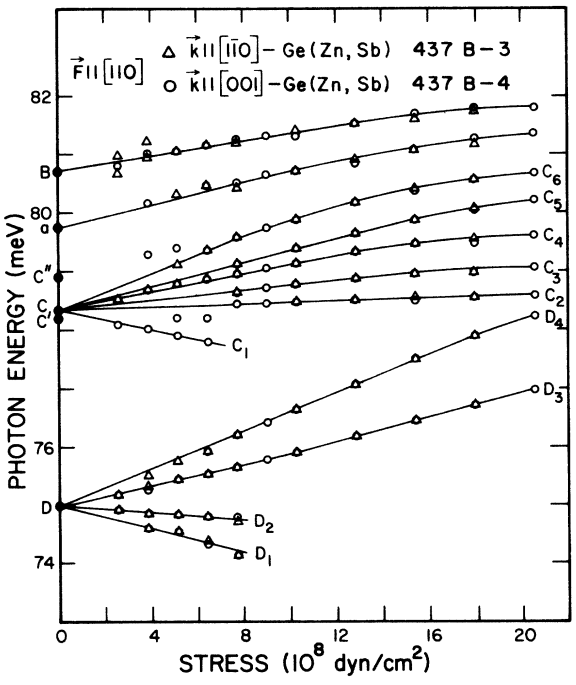


FIG. 21. Energies of the stress-induced components of the $B$, $a$, $C$, and $D$ lines for $\vec{F}\|[110]$ as a function of stress for both directions of $\vec{k}$.

the effect of interactions is unknown. This value is to be compared with $(0.80 \pm 0.03) \times 10^{-9} |S|$ predicted from the value of $\Delta^D_{100}$ given above and $\Delta^D_{111} = 0$. The ratio of $\Delta'_{110}$ to $\Delta^D_{110}$ obtained from Fig. 22 is 2.5, in good agreement with that given in II, and is to be compared with the value of $2.4 \pm 0.14$ obtained from the predicted values of $\Delta'_{110}$ and $\Delta^D_{110}$.

It is shown in I that, for $\vec{F} \| \langle 110 \rangle$, the intensities of the $D$ components depend upon the deformation-potential constants for both the ground state and the excited state, as well as $u_D$ and $v_D$. In Table XVIII of I, the intensities are given in terms of the quantities $\gamma$ and $\delta$ where $\gamma = x + (1+x^2)^{1/2}$ and $x = \Delta'_{100}/\sqrt{3}\,\Delta'_{111}$. The quantity $\delta$ is defined in the same manner, but for the excited state. We find that for the present values of $\Delta'_{100}$ and $\Delta'_{111}$, $\gamma = 1.68 \pm 0.05$, which is to be compared with the value of $1.62 \pm 0.03$ quoted in II. The change in $\gamma$ is not large enough to warrant a recalculation of the intensities for this direction of compression. The original calculation is particularly justified since the component $D_4^{\perp}$ for $\vec{k} \| [001]$ has now been observed. Further, as may be seen from Fig. 23, the component $D_2^{\perp}$ for $\vec{k} \| [1\bar{1}0]$ is actually the strongest component for this direction of polarization as was predicted in II. The other relative intensities observed in the present measurements for $\vec{F} \| \langle 110 \rangle$ are consistent with those calculated and observed in II.

#### 4. *Stress-induced components of the C, B, and a lines*

The results presented here show that the excited state associated with the $C$ line splits into at least four sublevels for $\vec{F} \| \langle 111 \rangle$ and into at least five sublevels for $\vec{F} \| \langle 100 \rangle$ and $\langle 110 \rangle$. In addition, there is some evidence that the $C''$ shoulder to the $C$ line arises from a separate level (see Fig. 15). This confirms the conclusion given in II that the excited state of the $C$ line is at least tenfold degenerate. Symmetry assignments may be made to some of the sublevels of the $C$ component by carrying the measurements to higher stresses and noting the identity of those components of known symmetry with which these sublevels interact. Such an experimental investigation may be difficult in view of the large number of relatively broad components which need to be separated.

For the $B$ and $a$ lines, at most one sublevel is observed for each and this clearly undergoes interaction effects, but the quality of the data is such that very little information about these two lines has been obtained.

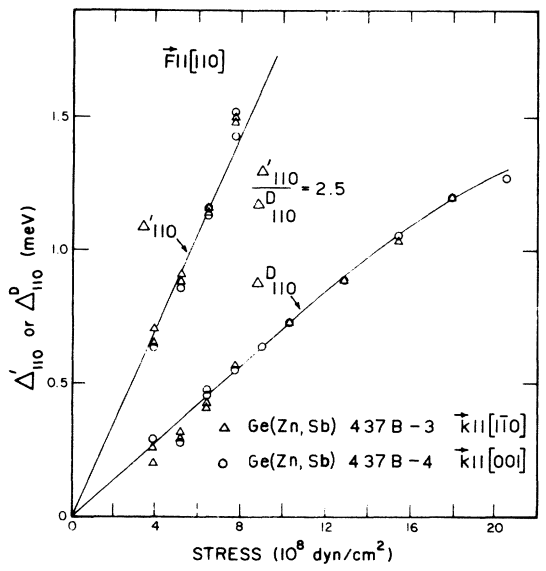


FIG. 22. $\Delta'_{110}$ and $\Delta^D_{110}$ as functions of stress.

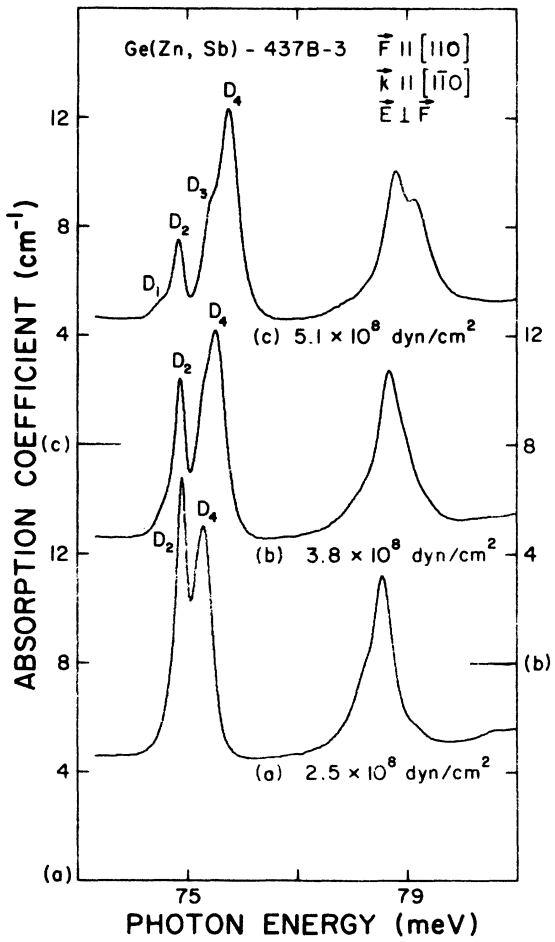


FIG. 23. Excitation spectrum of $Zn^-$ for three different small stresses with $\vec{F} \| [110]$, $\vec{k} \| [1\bar{1}0]$, and $\vec{E} \perp \vec{F}$.

## IV. CONCLUDING REMARKS

The present investigation has resulted in a complete verification of the theory of the $D$ transition as developed in I and II. The only remaining ambiguity in the data is the large variation in the value of $u_D$ obtained by estimating this parameter in different ways. However, there are many systematic errors associated with the measurement of intensities which might account for this discrepancy. The complex nature of the final state of the $C$ line has been confirmed by the need for at least five sublevels to understand the stress pattern.

Samples with different concentrations of $Zn^-$ used in this investigation indicated a definite trend for the energy of the $D$ line to depend on the concentration, with higher concentrations leading to higher energies. This effect may be associated with the asymmetry observed for all the lines. Although the $C$ line is the most remarkable example of this, all the lines show some asymmetry, with the low-energy side appearing broader than the high-energy side. For the sample of Fig. 1, for example, the low-energy side of the $D$ transition is about twice as wide as the high-energy side, as determined by the curve-fitting program, and the line has shifted to 75.002 meV, rather than the 74.994 meV found for the lower-concentration sample. Sidorov *et al.*[19] have reported that the $D$ line of $Zn^-$ occurs at an energy of $75.4 \pm 0.2$ meV in samples which apparently have higher $Zn^-$ concentration than the ones used here; this may be another manifestation of this effect.

There is little doubt that the most startling aspect of the present study has been the detection of the $G$ line. The spectacular way in which the stress components of this line grow is quite remarkable. It should be mentioned that there is some evidence[20] that the $G$ line of neutral copper in germanium[6] also undergoes dramatic stress enhancement. This effect is being further explored for copper and the other acceptors in germanium.

## ACKNOWLEDGMENTS

The authors wish to thank Professor A. K. Ramdas for a critical reading of the manuscript, along with Professor S. Rodriguez and Dr. H. R. Chandrasekhar for a number of stimulating discussions.

---

*Work supported by the NSF (GH32001A1 and MRL Programs GH33574A1 and GH33574A3).

†Present address: Radiation Center, Honeywell Inc., 2 Forbes Rd., Lexington, Mass. 02173.

‡Present address: Department of Physics, University of Wollongong, N.S.W., 2500, Australia.

[1]S. Rodriguez, P. Fisher, and F. Barra, Phys. Rev. B 5, 2219 (1972); this publication will be referred to as I. See also Erratum, Phys. Rev. B 7, 2889 (1973).

[2]F. Barra, P. Fisher, and S. Rodriguez, Phys. Rev. B 7, 5285 (1973); this publication will be referred to as II. See also Erratum, Phys. Rev. B 9, 2784 (1974).

[3]V. J. Tekippe, H. R. Chandrasekhar, P. Fisher, and A. K. Ramdas, Phys. Rev. B 6, 2348 (1973).

[4]N. R. Butler, Ph.D. thesis (Purdue University, 1974) (unpublished).

[5]A brief report on this has been given in N. R. Butler and P. Fisher, Bull. Am. Phys. Soc. 20, 385 (1975).

[6]P. Fisher and A. K. Ramdas, *Physics of the Solid State*, edited by S. Balakrishna, M. Krishnamurthi, and B. Ramachandra Rao (Academic, New York, 1959), p. 149.

[7]P. Fisher and H. Y. Fan, Phys. Rev. Lett. 5, 195 (1960).

[8]R. L. Jones and P. Fisher, J. Phys. Chem. Solids 26, 1125 (1965).

[9]A. K. Bhattacharjee and S. Rodriguez, Phys. Rev. B 6, 3836 (1972).

[10]Manufactured by Perkin-Elmer Corporation, Norwalk, Connecticut 06856.

[11]Manufactured by Santa Barbara Research Center, Goleta, California 93017.

[12]N. R. Butler and P. Fisher, Phys. Lett. A 47, 391 (1974).

[13]E. E. Haller and W. L. Hansen, Solid State Commun. 15, 687 (1974).

[14]Note that in Ref. 2, the energy of the $D$ line was inadvertently reported as 74.944 meV instead of the observed value of 74.994 meV, given in Table I.

[15]For the sample of Fig. 4, a value of $3.88 \pm 0.02$ was found for the refractive index of germanium at liquid helium temperature over the wavelength range 15–17 $\mu$. This is not in agreement with the value of 3.919 $\pm$ 0.005 predicted by Faulkner [R. A. Faulkner, Phys. Rev. 184, 713 (1969)]. The discrepancy, presumably, is because the present value is obtained for shorter wavelengths than are appropriate to the effective-mass calculation of binding energies.

[16]H. R. Chandrasekhar, P. Fisher, A. K. Ramdas, and S. Rodriguez, Phys. Rev. B 8, 3836 (1973).

[17]This effect was observed previously (see Fig. 5 in II) but was thought to be an experimental uncertainty.

[18]R. L. Aggarwal and A. K. Ramdas, Phys. Rev. 137, A602 (1965).

[19]V. I. Sidorov, T. E. Sushko, and A. Ya. Shul'man, Fiz. Tverd. Tela 8, 2022 (1966) [Sov. Phys.-Solid State 8, 1608 (1967)].

[20]R. L. Jones and P. Fisher (unpublished).